

High-pressure resistivity and thermoelectric power in $\text{Yb}_{14}\text{MnSb}_{11}$

A. Akrap,¹ N. Barišić,¹ L. Forró,¹ D. Mandrus,² and B. C. Sales²

¹*Institut de Physique de la matière complexe, EPFL, CH-1015 Lausanne, Switzerland*

²*Material Science and Technology Division, Oak Ridge National Laboratory, Oak Ridge, Tennessee 37831*

(Received 15 November 2006; revised manuscript received 14 May 2007; published 3 August 2007)

We report the electrical transport properties of $\text{Yb}_{14}\text{MnSb}_{11}$, resistivity and thermoelectric power under pressures up to 2.3 GPa. In both transport coefficients we can follow the ferromagnetic transition, which shows a shift from the ambient pressure value of 52 K to lower temperatures and eventually saturation at 49 K for $p > 2.0$ GPa. The high values of thermopower and its linear temperature dependence down to 100 K demonstrate that the system is a bad metal. Anomalies in the thermopower below the ferromagnetic transition are rather sensitive to pressure. Our experimental observations are consistent with the model of an underscreened Kondo lattice.

DOI: [10.1103/PhysRevB.76.085203](https://doi.org/10.1103/PhysRevB.76.085203)

PACS number(s): 75.30.Mb, 75.50.Pp

Bright prospects for the future applications of ferromagnetic semiconductors, for example, in detection and manipulation of magnetic signals,¹⁻³ motivate the research in a wider class of dilute magnetic systems. Among them, $\text{Yb}_{14}\text{MnSb}_{11}$ is a stoichiometric, natural dilute magnetic system, in which the magnetic sites are regularly positioned within the crystal lattice. Therefore this so-called 14-1-11 Zintl compound could serve as a model system for magnetic semiconductors. It was indicated by optical⁴ and Hall effect measurements⁵ that $\text{Yb}_{14}\text{MnSb}_{11}$ may be a rare example of a d -electron underscreened Kondo lattice. Moreover, it has recently been found that this compound is a highly efficient thermoelectric at high temperatures (975–1275 K), with an average figure of merit $ZT=0.95$, outperforming all the previously reported p -type thermoelectric materials.⁶

Manganese moments in $\text{Yb}_{14}\text{MnSb}_{11}$ are placed within the tetrahedra formed by Sb atoms and spaced about 10 Å apart,⁷ which is why their interaction is mediated by conducting holes [Ruderman-Kittel-Kasuya-Yosida (RKKY) interaction]. The Yb atoms are divalent and nonmagnetic.⁹ The manganese moments are only partially screened by mobile carriers, the $5p$ holes from the antimony bands. The Kondo temperature was estimated from the mass renormalization to be about 350 K. It should be noted, however, that there is no clear evidence of a Kondo peak in the resistivity in that temperature region.⁶ The optical measurements by Burch *et al.*⁴ showed that a coherence between the underscreened Mn moments appears as they order ferromagnetically at 52 K. Upon ordering, the entropy coming from the local magnetic moments is reduced by the change of the spectral weight of the d electrons from the incoherent local high-frequency part to the coherent low frequency response.¹⁰

The transport properties capture many features in the electronic structure of $\text{Yb}_{14}\text{MnSb}_{11}$, as well as its evolution under pressure. In this article we report high-pressure electrical transport measurements, resistivity, and thermoelectric power. Our main finding is the pressure-induced decrease of the onset temperature of ferromagnetic ordering, in contrast with the results obtained on, e.g., (In,Mn)Sb films.³ We show that the behavior of the resistivity and thermoelectric power may be consistent with the suggested Kondo lattice model.^{4,5} The drop which appears in both transport coefficients at the temperature of the ferromagnetic ordering and becomes more

pronounced under pressure, suggests that the coherence strengthens. Moreover, the pressure increases the effective mass.

In this study we used single crystal samples of $\text{Yb}_{14}\text{MnSb}_{11}$ prepared at Oak Ridge National Laboratory. Electrical transport measurements were done on several polished crystals of typical dimensions $3 \times 1 \times 0.5$ mm³. The crystals were not oriented because previous results indicated that the transport properties were not very anisotropic.⁸ A sample with four silver epoxy-glued contacts was mounted on a homemade thermopower sample holder, fitting into a Cu-Be clamped pressure cell. Small metallic heaters installed at both ends of the sample generated the temperature gradient, measured with a chromel-constantan differential thermocouple. We simultaneously measured the resistivity and the thermoelectric power. The measured values of thermopower were corrected for the contribution of the golden leads to the sample. The pressure dependence of the absolute thermopower of gold, chromel and constantan is small with respect to the sample $S(p)$; still, small pressure-induced changes in the thermopower of the sample should be interpreted carefully. The pressure medium used in this study was kerosene. A calibrated InSb pressure gauge served to determine the pressure.

The temperature and pressure dependence of the resistivity is shown in Fig. 1. At ambient pressure, a rather high value of resistivity (~ 1500 $\mu\Omega$ cm) at room temperature points to the fact that $\text{Yb}_{14}\text{MnSb}_{11}$ is either a bad metal, or a heavily doped semiconductor, with the acceptor band situated slightly above the valence band. The resistivity increases as pressure is applied. This might, for instance, be due to the effective mass enhancement or the electron scattering time shortening. The mean free path at ambient pressure, calculated knowing the carrier density $n=1.35 \times 10^{21}$ holes/cm³ determined by the Hall effect measurement,⁵ is $l \approx 7$ Å. This is significantly below the Ioffe-Regel limit, since the corresponding de Broglie wavelength is $\lambda_F \approx 17$ Å.

At temperature T_c , a ferromagnetically ordered phase is established, marked by a break in the slope of the resistivity curves. We note that above the T_c , the resistivity curves for all the pressures can be scaled onto each other. This suggests that it is not the scattering process (i.e., the relaxation rate)

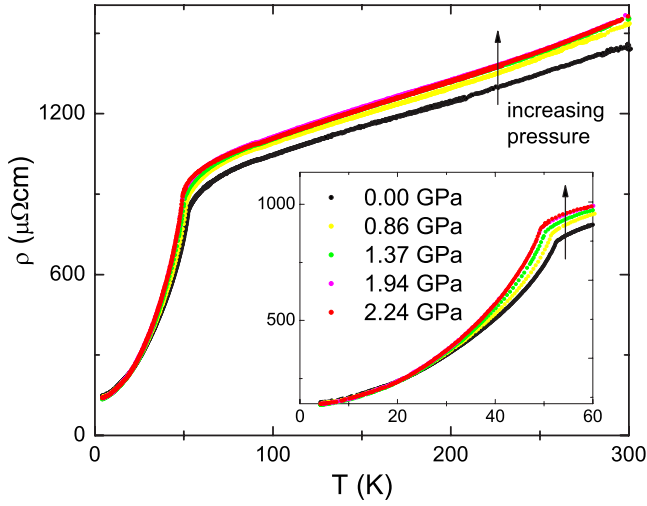


FIG. 1. (Color online) Resistivity of $\text{Yb}_{14}\text{MnSb}_{11}$ under various pressures. The arrows indicate the direction of increasing pressure. The initial linear temperature dependence goes down to 90 K. The ferromagnetic transition at about 50 K is marked by a sharp change in the slope and the beginning of T^2 dependence.

which is influenced by pressure. It is likely that the pressure enhances the effective mass. This seems also to be the case in (In,Mn)Sb dilute magnetic semiconductor.³ A similar increase in transport coefficients under pressure has been seen in some other ytterbium systems, particularly in the heavy fermion compounds (see, e.g., Ref. 11). It has also been observed in the pure Yb system up to about 4.0 GPa, where it was attributed to the decrease of overlap between Yb $6s$ and $6p$ bands.¹² These bands contribute to the conduction band in $\text{Yb}_{14}\text{MnSb}_{11}$.¹³ A pressure-induced increase in resistivity would also be consistent with a decrease in the concentration of holes.

The appearance of ferromagnetism is followed by an increase of the carrier concentration⁵ and the onset of the T^2 dependence of resistivity, characteristic of Fermi liquids

$$\rho = \rho_0 + AT^2. \quad (1)$$

The Kadowaki-Woods ratio A/γ^2 calculated using the specific heat data⁵ and the coefficient A from Eq. (1), equals $1.6 \times 10^{-5} \mu\Omega \text{ cm} (\text{mol K/mJ})^2$ for the ambient pressure. This is in the range of the values characteristic of heavy fermion compounds. Namely,

$$A/\gamma^2 \sim 10^{-5} \mu\Omega \text{ cm} (\text{mol K/mJ})^2$$

is known to hold for a variety of strongly correlated Fermi liquids. Residual resistivity ρ_0 in the Fermi liquid region is rather large, about $145 \mu\Omega \text{ cm}$ at ambient pressure, and it decreases slightly with pressure, down to $\sim 130 \mu\Omega \text{ cm}$, indicating that the coherence increases. Residual resistivity ratio thus grows from 9.9 at ambient pressure to 12.1 at 2.3 GPa. The coefficient A , plotted in Fig. 2, is enhanced by more than 20% under pressure. Its values are between 0.22 and $0.28 \mu\Omega \text{ cm K}^{-2}$. This again signifies an increase in correlation. As $A \propto (m^*/m)^2 \propto \gamma$, this reinforces our previous statement: the dominant effect of pressure is a change in the

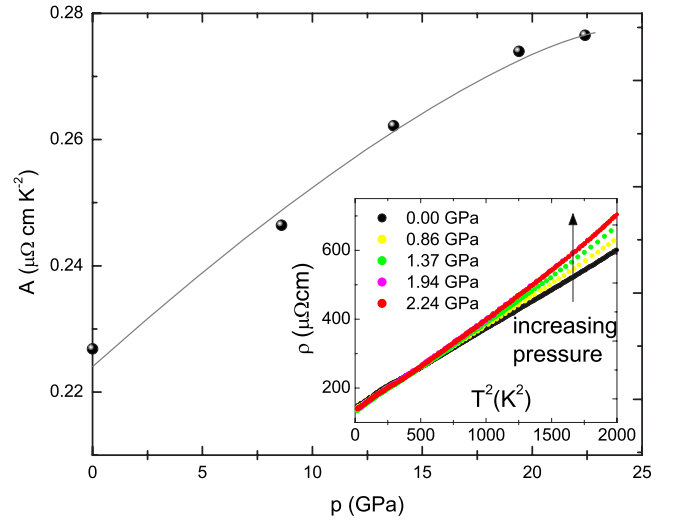


FIG. 2. (Color online) Pressure dependence of the coefficient A from the equation $\rho = \rho_0 + AT^2$. The inset shows the T^2 dependence of the resistivity in the ferromagnetic region. The direction of pressure increase is given by the arrow.

effective mass. We note that the thus implied effective mass increase is higher in the ferromagnetically ordered region of temperature.

However, because of the presence of long range magnetic order, it is possible that the T^2 term in the resistivity is caused by electrons scattering on spin waves.¹⁴ In this case, the enhancement of the coefficient A under pressure would mean that there should also be an increase in the exchange coupling between the Mn magnetic moments.

Finally, the origin of the T^2 dependence of the resistivity may be more complex than suggested above. It was found¹⁵ that replacing a small part of Yb atoms by La atoms leads to a T^3 dependence of the resistivity. This may imply that there are several contributions to the scattering in the ferromagnetically ordered phase of $\text{Yb}_{14}\text{MnSb}_{11}$.

A particularly interesting point is the decrease of T_c under pressure, which occurs at the rate of $\partial T_c / \partial p = -1.75 \text{ K/GPa}$. The interaction between Mn moments is ferromagnetic and mediated by conducting holes, so it can be described by the RKKY interaction. The corresponding exchange coefficient \mathcal{J} has a damped oscillatory nature, with the period of oscillation determined by the Fermi surface diameter. The magnetic coupling between a pair of ions can be ferromagnetic or antiferromagnetic, depending on their separation a_0 . By squeezing the lattice under pressure the Fermi vector k_F is, in the first approximation, neglecting the band structure change, proportionally increased, if the number of carriers is left unchanged. Since the positions of nodes of \mathcal{J} are determined by the product $k_F a_0$, the pressure only rescales the problem and does not account for the changes in the coupling strength.

One possibility of interpreting the shift of T_c to lower temperatures is to think of it in terms of the increase of Kondo screening effect with pressure. In many heavy fermion systems the interplay between nonmagnetic and magnetically ordered states depends on the competition between Kondo effect and RKKY interaction. These two interactions seem to be rather balanced in $\text{Yb}_{14}\text{MnSb}_{11}$, since both mag-

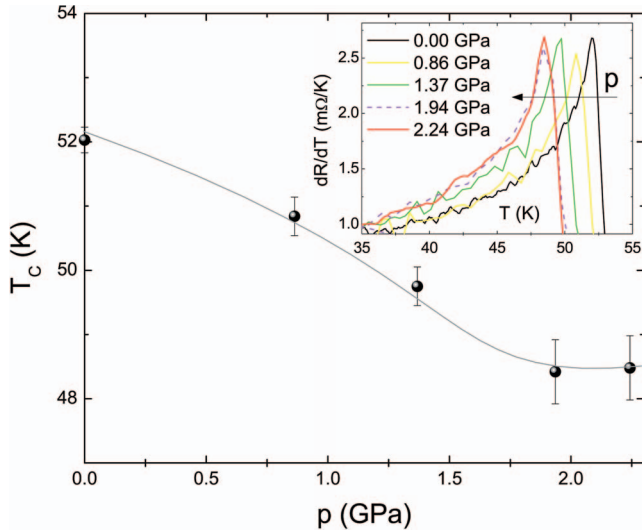


FIG. 3. (Color online) The temperature of ferromagnetic ordering vs pressure, as deduced from the resistivity curves. The inset shows the derivatives of resistivity for different pressures. The arrow indicates increasing pressure.

netic order and mass enhancement are observed. The hybridization between conduction electrons and the localized $3d$ electrons of Mn atoms might be responsible for both of these interactions. At ambient pressure, we are already in the region where $T_K > T_{RKKY}$. As the pressure increases, this hybridization gets stronger, along with the Kondo screening of conduction electrons. Screening being destructive to magnetic ordering, T_c decreases. Indeed, Fig. 3 bears resemblance to the part of Doniach's phase diagram¹⁶ in which Kondo screening dominates. Still, there is an important difference: the coupling in our case is ferromagnetic. Alternatively, one could attribute the decrease of T_c only to the weakening of interaction between Mn moments. Because the conduction band becomes narrower under pressure, which is evidenced in the increase of the high-temperature resistivity, the coupling of the carriers to the magnetic moments could be expected to decrease, which would have as a consequence a decrease of the Curie temperature. However, this seems to be at odds with the enhancement of the coefficient A under pressure.¹⁴

On the other hand, the observed decrease of the Curie temperature under pressure could also be explained within the Stoner-Wohlfarth theory of weak itinerant ferromagnetism.^{17,18} Such an effect was seen in a number of $3d$ element ferromagnetic metals.¹⁹ The temperature and pressure dependence of the resistivity of several such alloys, for example, NdCo_2 (Ref. 20) or Co_2TiAl ,²¹ shows qualitatively similar behavior to what we observe in $\text{Yb}_{14}\text{MnSb}_{11}$, although the T_c of the above compounds decreases at a significantly higher rate under pressure.

It is interesting to see how the ferromagnetic ordering influences another transport coefficient, the thermoelectric power. Figure 4 shows the evolution of the temperature dependence of the thermopower from ambient pressure to 2.3 GPa. This quantity is generally more sensitive than resistivity to the details of the Fermi surface. The pressure and temperature dependent behavior of thermopower confirms

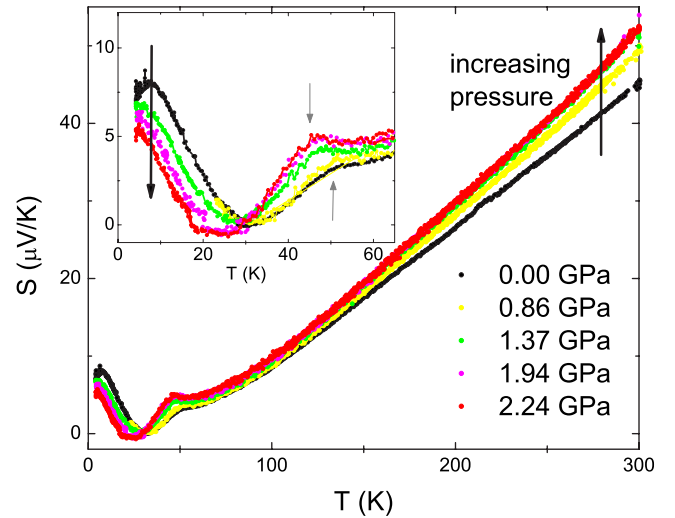


FIG. 4. (Color online) Thermoelectric power for different pressures, where the direction of increasing pressure is given by black arrows. The inset shows the peak (marked by gray arrows) which follows the ferromagnetic ordering and, under pressure, shifts from 52 to 48 K. A saturation is visible for $p > 2.0$ GPa in the high-temperature part of the inset.

some of our conclusions based on the resistivity. The high room-temperature value of TEP is in accord with the bad metallicity of $\text{Yb}_{14}\text{MnSb}_{11}$. From room temperature down to about 90 K the behavior of the thermopower is linear in temperature. According to the recent measurements by Brown *et al.*,⁶ the linearity extends to about 1000 K. In addition to the clear metallic behavior, there is a significant negative offset. Extrapolation to $T=0$ K gives $-10 \mu\text{V K}^{-1}$ at ambient pressure, which increases in magnitude under higher pressures. Let us consider the independent electron model, which describes thermopower by the two terms of the Boltzmann formula²³

$$S(T) = -\frac{\pi^2 k_B}{3|e|} k_B T \left[\frac{N(\epsilon_F)}{n} + \frac{1}{\tau(\epsilon_F)} \frac{d\tau}{d\epsilon_F} \right], \quad (2)$$

where $N(\epsilon_F)$ is the density of states at the Fermi level, n conduction electron density, and τ the relaxation time. The band structure depends weakly on temperature, the relaxation time presumably has a stronger dependence. Therefore, the above equation tells us that the linear behavior of the thermopower is related to the band structure, whereas the deviations from linearity have to do with the conduction mechanism, or with the fact that the Fermi energy changes with temperature. At higher temperatures we may assume that the relaxation time is independent of energy and we obtain

$$S(T) = -\frac{\pi^2 k_B^2 T}{2|e|E_F}. \quad (3)$$

This expression allows us to calculate the free electron value of Fermi energy. For the ambient pressure we get $E_F \approx 0.24$ eV, and for the highest pressure, 2.3 GPa, this value is slightly lowered: 0.21 eV. Pressure increases the room-

temperature value of TEP from about 47 to 55 $\mu\text{V K}^{-1}$. A pressure-induced modification of the density of states only multiplies the TEP by a factor, as stated above. Since in the high-temperature part of the thermopower curves only the slope changes with pressure, this confirms the increase of effective mass under pressure.

In the thermopower there is also a clear signature of the ferromagnetic ordering. At ambient pressure, the metallic part above 100 K is followed by a flat region between 90 K and the T_c . When the ferromagnetic ordering takes place, there is a sharp decrease towards the minimum value of thermopower at about 30 K. When pressure is applied, the shape of the anomaly at the ferromagnetic ordering evolves into a small peak, which shifts to lower temperatures. At low temperatures thermopower behavior becomes more complex. For the ambient pressure, below T_c the TEP reaches a local minimum, which within our experimental resolution falls to zero. At the very lowest temperatures measured, around 5 K, we observe the formation of a local maximum. Under pressure, the local minimum and the low-temperature peak are decreased in magnitude and shifted to lower temperatures. This kind of behavior in the thermopower probably results from the energy dependence of the relaxation time, which means the scattering is changed and the second term in Eq. (2) becomes important. The drop in the thermopower appearing just below the ferromagnetic ordering can be associated with the establishment of a coherence, which brings about a loss in scattering. The fact that this drop gets steeper under pressure might be explained by the strengthening of the Kondo effect and the increase in electronic coherence. This part of the TEP curve is, similarly to the T_c and within the experimental resolution, left unchanged from 1.9 to 2.3 GPa.

The lowest temperature features in thermopower seem more difficult to understand. One would tentatively ascribe either the minimum of the curve (appearing around 30 K) or the local maximum at 5 K to the phonon drag. This might

make sense at ambient pressure, since normally phonon drag appears between $\theta_D/10$ and $\theta_D/5$, where $\theta_D=160\pm 10$ K is the Debye temperature²² determined by specific heat measurements.⁸ However, since the characteristic temperature of both peaks shifts significantly to lower temperatures under applied pressure, this explanation would imply a decrease in θ_D under pressure, which is not only unlikely in this pressure range, but also unphysical. Moreover, the thermal conductivity of $\text{Yb}_{14}\text{MnSb}_{11}$ is low, as it was seen in the high temperature measurements by Brown *et al.*⁶ This means that the phonon mean free paths are short, probably limited by the complexity of the structure, which explains the absence of the phonon drag in thermopower. Finally, in the magnetic field of 8 T the low temperature part of the thermopower is enhanced,¹⁵ which is not in accord with a phonon drag mechanism. Instead, it seems reasonable that the rise in thermopower below 30 K at ambient pressure is related to the development of coherent quasiparticles, as was seen in the recent optical study.⁴

In conclusion, we have shown that the resistivity and thermoelectric power consistently display a shift of the ferromagnetic order to lower temperatures under pressure. Both quantities grow under pressure, scaling together. Coefficients extracted from the resistivity are in accord with the increase of coherence under pressure. Our experimental observations are consistent with the previously invoked model of under-screened Kondo lattice,^{4,5} and would suggest that the Kondo effect strengthens under pressure.

We gratefully acknowledge discussions with T. Fehér and B. Náfrádi. Part of research was sponsored by the Division of Materials Sciences and Engineering, Office of Basic Energy Sciences, U.S. Department of Energy, under Contract No. DE-AC05-00OR22725 with Oak Ridge National Laboratory, managed and operated by UT-Battelle, LLC. The work in Lausanne was supported by the Swiss National Science Foundation and its NCCR MaNEP.

-
- ¹M. Yamanouchi, D. Chiba, F. Matsukura, and H. Ohno, *Nature* (London) **428**, 539 (2004).
- ²D. Chiba, M. Yamanouchi, F. Matsukura, and H. Ohno, *Science* **301**, 943 (2003).
- ³M. Csontos, G. Mihaly, B. Janko, T. Wojtowicz, X. Liu, and J. K. Furdyna, *Nat. Mater.* **4**, 447 (2005).
- ⁴K. S. Burch, A. Schafgans, N. P. Butch, T. A. Sayles, M. B. Maple, B. C. Sales, D. Mandrus, and D. N. Basov, *Phys. Rev. Lett.* **95**, 046401 (2005).
- ⁵B. C. Sales, P. Khalifah, T. P. Enck, E. J. Nagler, R. E. Sykora, R. Jin, and D. Mandrus, *Phys. Rev. B* **72**, 205207 (2005).
- ⁶S. R. Brown, S. M. Kauzlarich, F. Gascoin, and G. J. Snyder, *Comput. Mater. Sci.* **18**, 1873 (2006).
- ⁷J. Y. Chan, M. M. Olmstead, S. M. Kauzlarich, and D. J. Webb, *Comput. Mater. Sci.* **10**, 3583 (1998).
- ⁸I. R. Fisher, T. A. Wiener, S. L. Budko, P. C. Canfield, J. Y. Chan, and S. M. Kauzlarich, *Phys. Rev. B* **59**, 13 829 (1999).
- ⁹A. P. Holm, S. M. Kauzlarich, S. A. Morton, G. D. Waddill, W. E. Pickett, and J. G. Tobin, *J. Am. Chem. Soc.* **124**, 9894 (2002).
- ¹⁰S. Nakatsuji, D. Pines, and Z. Fisk, *Phys. Rev. Lett.* **92**, 016401 (2004).
- ¹¹V. Zlatić, B. Horvatić, I. Milat, B. Coqblin, G. Czycholl, and C. Grenzebach, *Phys. Rev. B* **68**, 104432 (2003).
- ¹²P. C. Souers and G. Jura, *Science* **140**, 481 (1963).
- ¹³D. Sánchez-Portal, R. M. Martin, S. M. Kauzlarich, and W. E. Pickett, *Phys. Rev. B* **65**, 144414 (2002).
- ¹⁴T. Kasuya, *Prog. Theor. Phys.* **16**, 58 (1956).
- ¹⁵B. C. Sales (unpublished).
- ¹⁶S. Doniach, *Physica B* **91**, 231 (1977).
- ¹⁷E. C. Stoner and E. P. Wohlfarth, *Philos. Trans. R. Soc. London, Ser. A* **240**, 74 (1948).
- ¹⁸E. P. Wohlfarth, *Colloq. Int. C. N. R. S.* **240**, 74 (1969).
- ¹⁹D. Wagner and E. P. Wohlfarth, *J. Phys. F: Met. Phys.* **11**, 2417 (1981).
- ²⁰O. Syshchenko, T. Fujita, V. Sechovsky, M. Diviš, and H. Fujii, *J. Magn. Magn. Mater.* **226-230**, 1062 (2001).
- ²¹E. DiMasi, M. C. Aronson, and B. R. Coles, *Phys. Rev. B* **47**, 14301 (1993).
- ²²R. D. Barnard, *Thermoelectricity in Metals and Alloys* (Taylor & Francis, London, 1972).
- ²³J. McCarten, S. E. Brown, C. L. Seaman, and M. B. Maple, *Phys. Rev. B* **49**, 6400 (1994).